BPB Reports

Regular Article

A *PRNP*-Disrupted Human Neuroblastoma Cell Line and Its Stable Transformants Expressing Prion Protein Variants

Yuko Okemoto-Nakamura[*, a], Isei Tanida[a,b], Toshiyuki Yamaji[a], Kentaro Hanada[*, a], and Ken'ichi Hagiwara[a]

[a]*Department of Biochemistry and Cell Biology, National Institute of Infectious Diseases, Toyama 1–23–1, Shinjuku-ku, Tokyo, 162–8640, Japan;* [b]*Present address: Department of Cell Biology and Neuroscience, Juntendo University School of Medicine, Bunkyo-ku, Tokyo, 113–8421, Japan*

Received July 25, 2019; Accepted September 11, 2019

A key event in prion diseases is the conformational conversion of a cellular normal form of the prion protein (PrP^C) to disease-associated conformers (PrP^{Sc}). Polymorphisms or mutations in the human prion protein gene (*PRNP*) are associated with acquired or hereditary human prion diseases. When human prion protein (PrP) variants are characterized by cDNA expression systems in cultured cells, the endogenous prion protein may affect the behavior of ectopically expressed prion variants. To eliminate this issue, we herein created a *PRNP*-disrupted mutant cell line from human neuroblastoma BE(2)-M17 cells. No morphological differences were observed between *PRNP*-null and parental cells. We stably introduced cDNAs encoding E196K-PrP and E200K-PrP (both of which are Creutzfeldt-Jakob disease (CJD)-related mutants), a non-pathogenic E219K-PrP, and wild-type control PrP into *PRNP*-null mutant cells using the PiggyBac system, and found that the glycosylation pattern of E196K-PrP differed from that of other PrPs. We also found that non-glycosylated PrPs for E196K- and E200K-PrPs had distinct electrophoretic mobilities from that of WT-PrP, and E219K-PrPs exhibited slightly different mobilities in polyacrylamide gel electrophoresis under endogenous PrP-null conditions, demonstrating that the *PRNP*-disrupted human neuroblastoma cell line serves as a useful tool for examining PrPs with mutations or polymorphisms.

Key words prion protein, CRISPR/Cas9, *PRNP* mutation, human neuroblastoma, Creutzfeldt-Jakob disease

INTRODUCTION

Transmissible spongiform encephalopathies (TSEs), or prion diseases, are fatal neurodegenerative diseases that affect several mammalian species, including humans. The causative infectious agents are prions, which are aggregates of the disease-associated forms of the prion protein (PrP^{Sc}; PrP denotes the prion protein). PrP^{Sc} is a conformational isoform of the non-pathogenic cellular prion protein (PrP^C), an *N*-glycosylated and glycosylphosphatidylinositol (GPI)-anchored membrane protein expressed in normal humans and animals.[1] The conformational conversion of PrP^C to PrP^{Sc} is a key process in the propagation of prions, and the molecular mechanisms responsible for this conversion remain controversial. In humans, TSEs are found as sporadic, acquired, or hereditary diseases, such as Creutzfeldt-Jakob disease (CJD), Gerstmann-Sträussler-Scheinker disease, fatal familial insomnia, kuru, and variant CJD, in which the conversion of PrP^C to PrP^{Sc} is initiated by an unknown etiological background or exposure to exogenous prions, or due to mutations in the *PRNP* gene encoding PrP, which is located on chromosome 20 in the human genome.

In most studies performed to date, ectopically expressed human prion proteins have been characterized in mammalian host cells in the presence of the endogenous wild-type (WT) prion protein gene.[2] However, difficulties are associated with specifically distinguishing ectopic PrPs from background signals by endogenous PrP; the precursor form of PrP has a membrane-translocating signal sequence at the N terminus and a GPI-anchoring signal sequence at the C terminus, both of which are cleaved off during maturation (UniProt access no. P04156), thereby preventing PrPs being added by epitope tags at either the N or C terminus. Furthermore, endogenous PrPs may affect the behavior of ectopically expressed PrPs of interest. To date, PrP-disrupted human cell lines have not been reported, although PrP gene-disrupted murine cells have been established for the analysis of PrP functions.[3,4] To overcome these issues, we herein constructed a *PRNP*-disrupted cell line from human neuroblastoma BE(2)-M17 cells using a clustered regularly interspaced short palindromic repeats (CRISPR)/CRISPR-associated protein-9 (Cas9) system. Within the *PRNP*-disrupted human neuroblastoma cell line, we examined the biochemical properties of two human PrP variants associated with hereditary CJD cases[5–9]: one has the substitution of Glu^{196} to Lys (referred to as E196K), and another has the substitution of Glu^{200} to Lys (referred to as E200K).

MATERIALS AND METHODS

Cell Line, Cell Culture, and Transfection of Plasmids The human neuroblastoma cell line BE(2)M-17 was purchased from the European Collection of Authenticated Cell Cultures

*To whom correspondence should be addressed. e-mail: yunaka@nih.go.jp; hanak@nih.go.jp

(ECACC: 95011816) and maintained in normal growth medium consisting of high-glucose Dulbecco's modified Eagle's medium (Fujifilm Wako Pure Chemical Co., Osaka, Japan) supplemented with 10% fetal bovine serum (Nichirei Bioscience Inc., Tokyo, Japan), 1% non-essential amino acids (Fujifilm Wako Pure Chemical Co.), and penicillin-streptomycin (Fujifilm Wako Pure Chemical Co.). Cells were detached by AccuMax dissociation solution (Innovative Cell Technologies, CA, USA) and passaged at a split ratio of 1:5. Lipofectamine®2000 reagent (Thermo Fisher Scientific, MA, USA) was used for the transfection of plasmids to cells.

Design of Single-Guide RNAs (sgRNAs) Targeting *PRNP* and the Construction of a Vector for the CRISPR/Cas9 System The plasmid pX330-U6-Chimeric_BB-CBh-hSpCas9, which expresses humanized Cas9 was a gift from Feng Zhang (Addgene plasmid #42230; http://n2t.net/addgene: 42230; RRID: Addgene_42230).[10] sgRNAs were designed using the freeware ZiFiT (http://zifit.partners.org/ZiFiT/ChoiceMenu.aspx) and synthesized with BbsI overhangs (Eurofins Genomics, Tokyo, Japan) (Fig. 1A); a pair of oligonucleotides 5'-CAC CTA GTA ATT TCA ACA TAA ATA-3' and 5'-AAA CTA TTT ATG TTG AAA TTA CTA-3' for the Target site A, and a pair of oligonucleotides 5'-CAC CGG ACC ATG CTC GAT CCT CTC-3' and 5'-AAA CGA GAG GAT CGA GCA TGG TCC-3' for the Target site B. They were phosphorylated by T4 polynucleotide kinase (New England Biolabs, MA, USA), annealed, and ligated to the BbsI site of pX330-U6-Chimeric_BB-CBh-hSpCas9.

Generation of *PRNP*-Disrupted Cells pX330-U6-Chimeric_BB-CBh-hSpCas9 for Target site A and that for Target site B were co-transfected with pSELECT-puro-mcs (InvivoGen, CA, USA) into BE(2)-M17 cells. After culturing transfected cells in normal growth medium supplemented with 2.5 μg/mL of puromycin (Takara Bio Inc., Shiga, Japan) for one week, viable cells were subjected to double serial dilutions followed by single cell isolation using fluorescence-activated cell sorting (FACS) with the FACSAria III machine (BD Biosciences, NJ, USA) for the absence of PrP expression on the cell surface stained by the mouse monoclonal anti-PrP antibody 6H4 (Roche Diagnostics, Basel, Switzerland), which reacts with the PrPs of various mammalian species. The established cell line, named BE(2)-K-041, was maintained in normal growth medium.

PCR Analysis and DNA Sequencing of *PRNP* Genomic DNA was isolated from cells using NucleoSpin Tissue (Takara Bio Inc.). A polymerase chain reaction (PCR) was performed using the following primers: primer set-1 (primer 1-Fw; 5'-CCT AGG GTA CAG CAG GTA CTG TTT AG-3', primer 1-Rv; 5'-TCT CAG GTC TAC TCT ATG TTT TCC AGT-3', both of which are outside of the region flanked by Target sites A and B), and primer set-2 (primer 2-Fw; 5'-GAG CAG GCC CAT CAT ACA TT-3', primer 2-Rv; 5'-TCC CTC TCG TAC TGG GTG AT-3', both of which are within the open reading frame (ORF) of *PRNP*) (Fig. 1A). PCR products by primer set-1 were subjected to a DNA sequence analysis.

Flow Cytometric Analysis Cells were detached by AccuMax and treated with the anti-PrP antibody 6H4, or the mouse immunoglobulin G1 (IgG1) isotype control, which lacks specific target binding (MEDICAL & BIOLOGICAL LABORATORIES CO., Aichi, Japan), in phosphate-buffered saline (PBS) at 4°C for 30 min. After washing with PBS, cells were incubated with an Alexa Fluor 488-conjugated goat anti-mouse IgG antibody (Thermo Fisher Scientific) in PBS at 4°C for 30 min. Cells were washed with PBS and analyzed with a FACSCalibur flow cytometer (BD Biosciences).

Stable and Transient Expression of PrPs in Cells The cDNA of human WT-PrP was obtained from the genomic DNA of BE(2)-M17 cells by PCR. The cDNAs for mutants (E196K-, E200K-, and E219K-PrPs) were generated by mutagenesis using the PrimeSTAR Mutagenesis Basal Kit (Takara Bio Inc). The mutagenic primers for E196K; 5'-AAG GGG AAG AAC TTC ACC GAG ACC GAC-3' and 5'-GAA GTT CTT CCC CTT GGT GGT TGT GGT-3', for E200K; 5'-CTT CAC CAA GAC CGA CGT TAA GAT GA-3' and 5'-TCG GTC TTG GTG AAG TTC TCC CCC TT-3', and for E219K; 5'-CCA GTA CAA GAG GGA ATC TCA GGC CTA-3' and 5'-TCC CTC TTG TAC TGG GTG ATA CAC ATC-3' were used, respectively. To obtain cells that stably express WT-PrP and mutant PrPs, the corresponding cDNAs were cloned into the PiggyBac Dual Promoter Vector PB514B-1 (System Biosciences, LLC, CA, USA), in which one promoter drives PrP gene expression and another promoter drives a puromycin resistance gene (pur^r) and a red fluorescent protein (RFP) gene bicistronically. Vectors were co-transfected with the Super PiggyBac Transposase Expression Vector (System Biosciences, LLC) for the integration of a *cDNA-*pur^r-RFP transposon cassette into the genome.[11,12] Cells were grown in normal growth medium supplemented with 4 μg/mL of puromycin, and sorted for RFP expression with FACSAria III to obtain cells, in which the *cDNA-*pur^r-RFP transposon cassette was integrated into the genome. The empty vector PB514B-1 was used as "MOCK".

Regarding the transient expression of non-glycosylated PrP, cDNA was mutagenized to change *N*-glycosylation sites (Asn^{181} and Asn^{197}) to Thr (N181T and N197T). The mutagenic primers for N181T were 5'-TGC GTC ACC ATC ACA ATC AAG CAG CAC-3' and 5'-TGT GAT GGT GAC GCA GTC GTG CAC AAA-3'. The primers for N197T mutagenesis in WT- and E219K-PrPs were 5'-GGG GAG ACC TTC ACC GAG ACC GAC GTT-3' and 5'-GGT GAA GGT CTC CCC CTT GGT GGT TGT-3'. The primers for N197T mutagenesis in E196K-PrP were 5'-AAG GGG AAG ACC TTC ACC GAG ACC GAC-3' and 5'-GAA GGT CTT CCC CTT GGT GGT TGT GGT-3', and the primers for N197T mutagenesis in E200K-PrP were 5'-GGG GAG ACC TTC ACC AAG ACC GAC GTT-3' and 5'-GGT GAA GGT CTC CCC CTT GGT GGT TGT-3'. cDNAs were cloned into PB514B-1, and transfected into cells without the Super PiggyBac Transposase Expression Vector. After cultivation for 48 h without puromycin, the transfected cells were subjected to Western blotting analysis.

Methionine and valine at codon 129 are polymorphic variations associated with susceptibility to prions.[13] Throughout the present study, we used the cDNA of *PRNP*, which encodes methionine (M) at codon 129.

Microscopic Analysis Live cells were observed under the BZ-8000 microscope (Keyence Co., Osaka, Japan) and analyzed using BZ Analyzer (Keyence Co.) software. In the immunofluorescent analysis of PrPs, cells were fixed with PBS containing 4% paraformaldehyde at room temperature for 10 min, and permeabilized with PBS containing 0.1% Triton X-100. After a 3-hour incubation with 1.0 μg/mL of the mouse monoclonal anti-PrP antibody SAF 32 (Cayman Chemical, MI, USA), which is preferentially used in immunocytochemis-

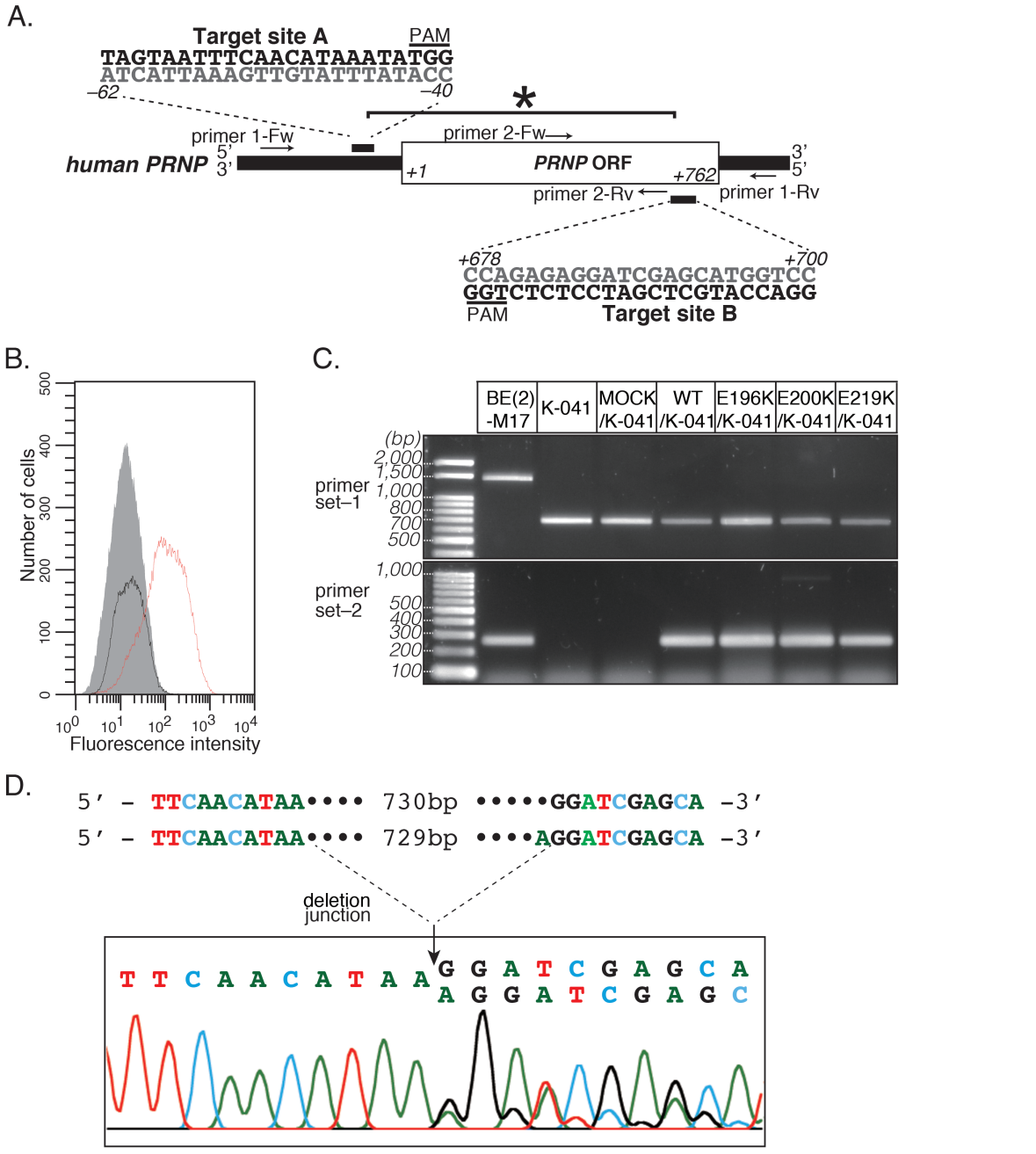

Fig. 1. Dual sgRNA-Guided Deletion of *PRNP*

(A) Target site A (the 5'UTR of *PRNP*) and Target site B (the 3'-end of ORF) are shown. Both targets have the 5′-TGG-3′ protospacer adjacent motif (PAM). Primer set-1 (primers 1-Fw and 1-Rv) is on the outside of the expected deletion regions, while primer set-2 (primers 2-Fw and 2-Rv) is in the sequence flanked by Target sites A and B. *; corresponding to the deletion site shown in (D). (B) A flow cytometric analysis of K-041 cells stained by the anti-PrP 6H4 antibody. Red; BE(2)-M17. Black; K-041. Shade; BE(2)-M17 stained with the isotype control IgG1 (negative control). (C) PCR analysis of genomic DNA. Primer set-1 amplified *PRNP* in the genome of BE(2)-M17 cells or detected the deletion of endogenous *PRNP* in K-041 cells. Primer set-2 could amplify not only *PRNP* in the genome of BE(2)-M17 cells, but also WT- or mutant *PRNP* integrated into the genome of transformants. (D) A DNA sequence analysis of *PRNP* in K-041 cells identified two deletions of 730 and 729 bp in length. This difference was attributed to the presence or absence of a single adenine at the deletion junction.

try, and a 1-hour incubation with 0.8 µg/mL of the Alexa Fluor 488-conjugated anti-mouse IgG secondary antibody (Thermo Fisher Scientific), cells were observed using the laser scanning confocal microscope LSM 700 (Zeiss, Oberkochen, Germany) with ZEN 2011 software (Zeiss).

Western Blot Analysis All manipulations were performed on ice or at 4°C unless otherwise noted. Cells were incubated in 100 mM Tris-HCl (pH 7.0) buffer containing 0.5% NP-40, 0.5% sodium deoxycholate, 10 mM ethylenediaminetetraacetic acid (EDTA), and 100 mM NaCl (hereafter referred to as NP40-DOC buffer) for 15 min for lysis. After centrifugation at 1,000×*g* for 5 min, supernatants were collected and protein concentrations were measured using a bicinchoninic acid (BCA) protein assay kit (Takara Bio Inc.). Proteins were precipitated in 4 volumes of ice-cold acetone by centrifugation at 20,000×*g* for 30 min. Air-dried pellets were dissolved in sodium dodecyl sulfate (SDS) loading buffer (3% SDS, 3 M urea, 100 mM dithiothreitol (DTT), 5% glycerol,

0.04% bromophenol blue, 3 mM EDTA, and 62.5 mM Tris-HCl, pH 6.8) and boiled for 10 min. Regarding the removal of *N*-linked glycans, samples were treated with peptide-*N*-glycosidase F (PNGase F) (New England Biolabs) according to the manufacturer's instructions. Briefly, 20 μg of protein in the denaturing buffer (0.5% SDS and 40 mM DTT) was denatured by heating for 10 min at 100°C, and incubated for overnight at 37°C with 500 units of PNGase F in the reaction buffer (0.5% SDS, 40 mM DTT, 1% NP-40 and 50mM sodium phosphate, pH 6.0). Samples were subjected to SDS-polyacrylamide gel electrophoresis (SDS-PAGE) using 15% e-PAGEL gels (ATTO Co., Tokyo, Japan) and Tris-glycine EzRun buffer (ATTO Co.), and transferred to polyvinylidene difluoride membranes (ATTO Co.). The primary and secondly antibodies used were the anti-PrP antibody 3F4 (BioLegend, CA, USA) (0.5 μg/mL) in Can Get Signal Immunoreaction Enhancer Solution (TOYOBO Life Science, Osaka, Japan), and a horseradish peroxidase-labeled (HRP-labeled) anti-mouse IgG antibody (Jackson ImmunoResearch, PA, USA) (0.7 μg/mL) in Tris-buffered saline with 0.05% Tween 20. Proteins were detected by Immobilon Western Chemiluminescent HRP Substrate (Merck Millipore, MA, USA) and a LAS-3000 mini chemiluminescence imaging system (Fujifilm, Tokyo, Japan) with ImageGauge software (Fujifilm). To ensure equivalent amounts of proteins were applied onto the gels (i.e., loading control), the membranes were reprobed with anti-glyceraldehyde-3-phosphate dehydrogenase (GAPDH) antibody (Enzo Life Sciences, NY, USA) in Can Get Signal Immunoreaction Enhancer Solution and processed in a similar way as described above.

Denaturing of PrPs by Guanidinium Chloride (GdnHCl), Urea, or Trichloroacetic Acid (TCA) After cell lysis with NP40-DOC buffer, lysates were added to urea (final concentration, 4 M), incubated at room temperature for 2 h, and boiled for 10 min in SDS loading buffer. Alternatively, lysates were added to equal volumes of 6 M GdnHCl, incubated at room temperature for 5 min, and diluted with 5 volumes of distilled water. Proteins were precipitated by the addition of 10 volumes of 10% TCA-acetone.

Regarding the pretreatment of cells with TCA, cells in 12-well plates were washed with PBS and incubated on ice with 10% TCA for 30 min. After washing 5 times with distilled water, cells were dissolved in NP40-DOC buffer. Samples were sonicated and centrifuged at 10,000×*g* for 1 min to precipitate debris. Protein concentrations in the supernatant were measured by the BCA assay, and proteins in the supernatant were precipitated by the addition of ice-cold acetone and centrifugation at 10,000×*g* for 30 min.

RESULTS AND DISCUSSION

Establishment of a *PRNP*-Disrupted Human Neuroblastoma Cell Line To disrupt the *PRNP* gene in human neuroblastoma BE(2)-M17 cells, we designed sgRNAs corresponding to a 5'-untranslated region (5'-UTR) of *PRNP* (Target site A) and the 3'-region in ORF (Target site B) (Fig. 1A). Cells were co-transfected with the pSELECT-puro-mcs plasmid (see Materials and methods). After selection by puromycin, cells were subjected to a limiting dilution and screening by FACS, and a clonal cell line named BE(2)-K-041 (which is hereafter referred to as K-041 for simplicity) was obtained. In the FACS analysis with the anti-prion monoclonal antibody 6H4, parental BE(2)-M17 cells exhibited a positive signal (Fig. 1B, red line) relative to the negative control experiment with the IgG1 isotype control, which has no known specificity (Fig. 1B, shaded area). This was consistent with the BE(2)-M17 cell genome having WT *PRNP* alleles. In contrast, K-041 cells exhibited no discernible positive signal (Fig. 1B black line), which almost overlapped with the signal observed for BE(2)-M17 cells stained with the negative control IgG1 (Fig. 1B, shaded area). *PRNP* alleles in the parental BE(2)-M17 cell line were found to be heterologous, encoding Met and Val at codon 129. It should also be noteworthy that K-041 cells are sensitive to puromycin, probably because the pSELECT-puro-mcs plasmid initially co-transfected was spontaneous eliminated during the establishment of the cell line.

A genomic PCR analysis demonstrated the occurrence of ~0.7-kbp deletions of the *PRNP* gene in the genome of K-041 cells (Fig. 1C, upper panel), which is consistent with the length of the genome between Target sites A and B. The sequencing of PCR amplicons by the Sanger method confirmed the deletion site(s), and identified two different deletions with lengths of 730 and 729 bp, both of which included the initiation codon (ATG) of *PRNP* (Fig. 1D). Using primer set-2 (Fig. 1A), no PCR product was obtained from K-041 (Fig. 1C, lower panel), ensuring the deletions in this region of the two different *PRNP* alleles (Fig. 1A). K-041 showed no marked changes in viability or morphology from parental BE(2)-M17 (see also below). This was consistent with previous findings showing no overt phenotypes in mice that lacked the prion protein gene (*Prnp*),[14,15] and no apparent defect in the growth of neuronal cells established from *Prnp*-knockout mice.[16]

Stable Transformants of K-041 Cells with Human PrP Variants The precursor of human PrP^C is composed of 253 amino acids, and the mature form consists of the amino acid sequence Lys^{23}-Ser^{230} from the precursor. More than fifty types of mutations (amino acid substitutions, repetition, and truncation) have been associated with hereditary human prion diseases.[5–7] The substitution of Glu^{200} to Lys (referred to as E200K) is linked to clusters of CJD patients in particular regions in the world,[8,9] while the substitution of Glu^{196} to Lys (referred to as E196K) has been identified in hereditary cases of CJD.[17] The existence of patients with heterozygotic alleles suggests that E200K and E196K both have dominant effects.[8,9,17,18]

To obtain K-041 transformants that stably express various types of human PrP variants, K-041 cells were transfected by PB514B-1 vectors that contained the cDNAs of WT-, E196K-, E200K-, and E219K-PrPs, together with the Super PiggyBac Transposase Expression Vector. After passages in medium containing puromycin (4 μg/mL), cells were sorted by FACS for the RFP signal derived from PB514B-1. The resultant bulk populations of RFP-positive cells were named MOCK/K-041, WT/K-041, E196K/K-041, E200K/K-041, and E219K/K-041, respectively, although they were not clonally purified. Stable expression of RFP after 30 passages in each cell population was confirmed with fluorescence microscopy (Fig. 2A right panels). In the PCR analysis with primer set-1 (Fig. 1A), these cells yielded ~0.7-kbp amplicons, which provided proof of the deletion of endogenous *PRNP* (Fig. 1C). PCR with primer set-2 (Fig. 1A) yielded ~0.3-kbp amplicons in WT/K-041, E196K/K-041, E200K/ K-041, and E219K/K-041 (Fig 1C lower panel), supporting integrations of the cDNA of WT-, E196K-, E200K-, and E219K-PrP into the genome.

BE(2)-M17, K-041, and these K-041-derived stable trans-

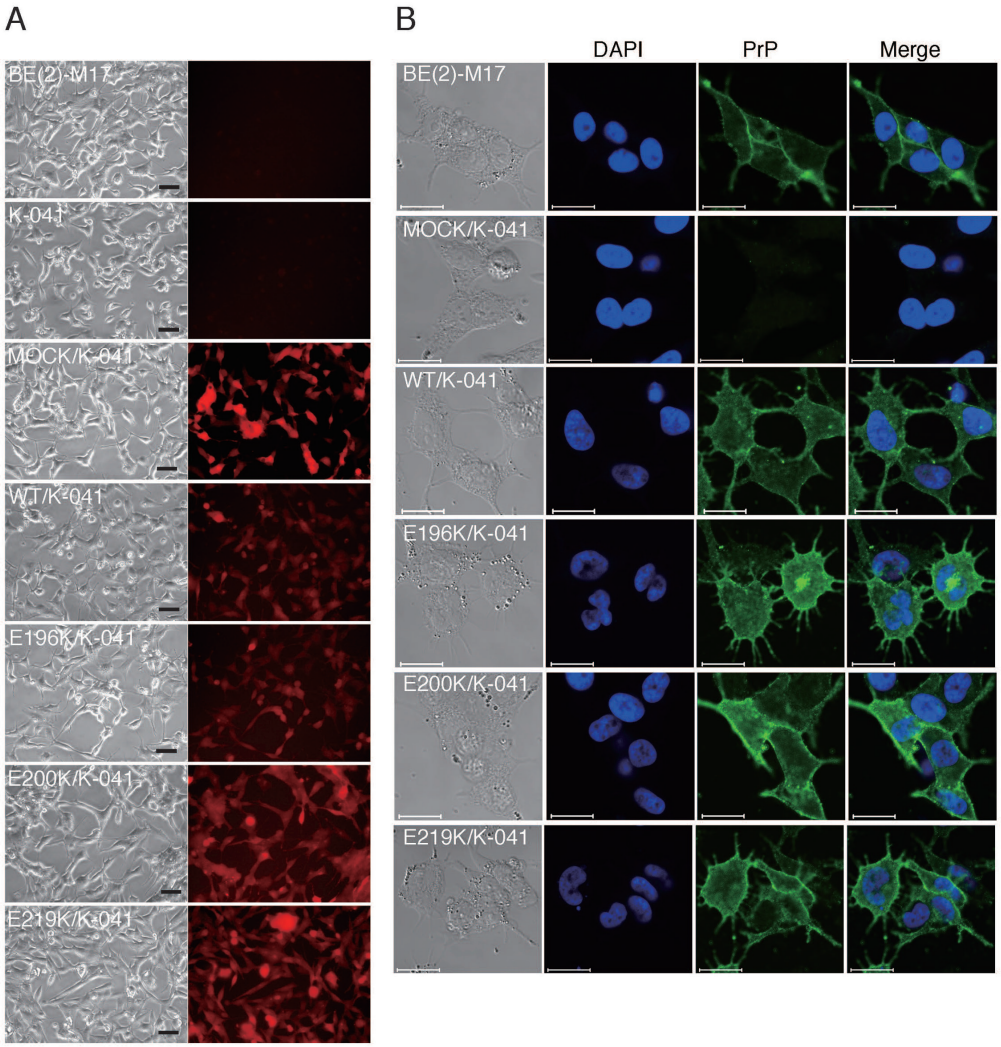

Fig. 2. Morphology and Immunofluorescent Analysis of Cells

(A) Morphology of cells under phase-contrast microscopy and RFP signals in WT- or mutant PrP/K-041 cells. No significant morphological difference was observed in K-041 cells transfected with an empty PB514B-1 vector (MOCK) and vectors having the cDNAs of WT-, E196K-, E200K-, and E219K-PrPs. BE(2)-M17 cells showed a similar morphology (left panels). Bars indicate 50 µm. After 30 passages, RFP signals (right panels) in MOCK, WT, E196K, E200K, and E219K/K-041 cell populations were confirmed, which indicate that each *cDNA-pur*-RFP transposon cassette are stably integrated into the genome of K-041. K-041 and BE(2)-M17 cells are negative for RFP signal. (B) Immunofluorescent analysis of WT- and mutant PrPs to demonstrate the subcellular localization of PrPs under confocal microscopy using the SAF 32 antibody (see Materials and methods). WT-PrP and E-to-K mutant PrPs mainly localized at the cell surface, similar to endogenous PrP in BE(2)-M17 cells. Bars indicate 20 µm.

formants showed no marked morphological differences under phase-contrast microscopy (Fig. 2A). In an immunocytochemical analysis of permeabilized cells by confocal microscopy, all of the ectopically expressed PrP variants were largely localized on the cell surface, while some dotted signals of PrP were observed in the cytosol (Fig. 2B). The intracellular localization patterns of the PrP variants were almost identical to the pattern of WT-PrP in K-041 cells and that of endogenous WT-PrP in BE(2)-M17 cells.

Biochemical Characterization of E-to-K PrP Mutants Expressed in K-041 Cells PrP is post-translationally modified at two potential *N*-glycosylation sites (-Asn^{181}-Ile-Thr- and -Asn^{197}-Phe-Thr-),[19] and it was demonstrated that the *N*-glycans attached to PrP are divergent with more than 400 different PrP glycoforms[20] although the contribution of *N*-glycans to metabolism and cellular localization of PrP^{C} remain enigmatic.[21,22] In the Western blot analysis after SDS-PAGE, WT-PrP and E219K-PrP showed similar glycosylation patterns: their di-glycosylated forms were more abundant than the non- and mono-glycosylated forms (Fig. 3A). In contrast, the mono-glycosylated form was found to be more abundant than the two other forms in E196K-PrP, and the non-glycosylated forms were the most abundant form in E200K-PrP (Fig. 3A). The difference in the glycosylation pattern of E196K may be, at least partly, attributed to the substitution of E196K potentially affecting glycosylation at the adjacent Asn^{197}. Notably, the substitution of Phe^{198} to Ser (which is a CJD-relevant mutation occurring next to Asn^{197}) was reported to induce an altered glycosylation pattern of PrP.[23] Previous studies showed that E200K-PrP exogenously expressed in M-17 BE(2)C cells exhibited different metabolism to that of WT-PrP due to the difference in the glycoforms between WT and E200K.[7,24]

We then investigated the mobility of the non-glycosylated forms of these PrPs in SDS-PAGE after the removal of *N*-glycans with PNGase F. The non-glycosylated forms from endogenous PrP in parental BE(2)-M17 cells and ectopically expressed WT-PrP in K-041 cells migrated identically in SDS-PAGE, displaying their relative molecular weight

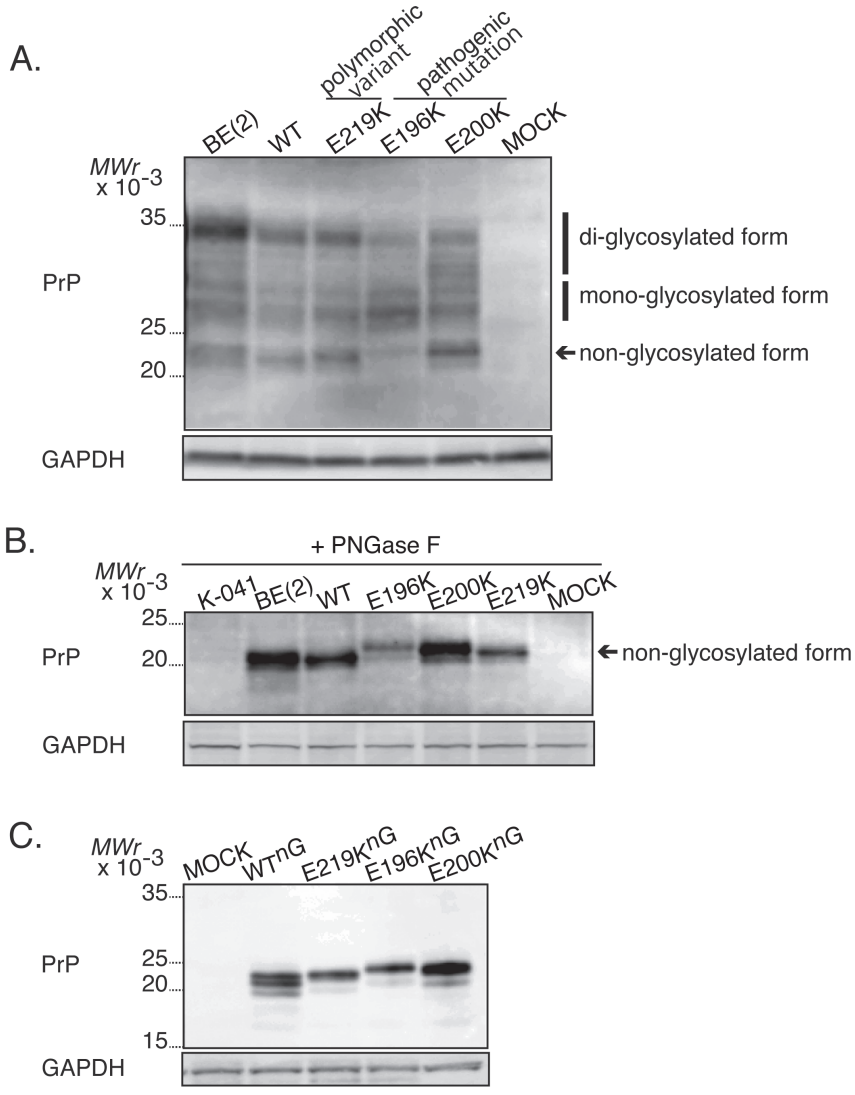

Fig. 3. Western Blot Analysis of PrPs

(A) Twenty-five-microgram aliquots of protein samples of bulk cell populations which stably expressed WT-PrP or mutant PrPs were subjected to a Western blot analysis using the anti-PrP antibody 3F4 (upper panel). Anti-GAPDH antibody was used as a loading control (lower panel). (B) Analysis of non-glycosylated PrPs. *N*-glycans of endogenous PrP (BE(2)), WT-PrP (WT), and mutant PrPs (E196K, E200K, and E219K) were removed by PNGase F. Five-microgram aliquots of protein samples were subjected to a Western blot analysis and detected by 3F4 antibody (upper panel) or anti-GAPDH antibody (lower panel). The variation of the expression levels or the mobility shifts caused by *PRNP* mutation were observed although little is known about the details of the metabolism or conformation of mutant PrPs. (C) Electrophoretic mobility of glycosylation-deficient mutants. In these mutants, glycosylation sites (Asn^{181} and Asn^{197}) were replaced by Thr. These glycosylation mutants were transiently expressed in K-041 cells. Fifteen-microgram aliquots of protein samples were subjected to a Western blot analysis using 3F4 antibody (upper panel) or anti-GAPDH antibody (lower panel). *MWr*; relative molecular weight.

(*MWr)* ~20,000 (Fig. 3B). On the other hand, non-glycosylated PrPs derived from the mutants (E196K-PrP, E200K-PrP, and E219K-PrP) displayed their *MWr* ~22,000. E196K-PrP, E200K-PrP migrated slightly faster than E219K-PrP (Fig. 3B). To confirm variant-dependent differences in mobility, we constructed cDNAs encoding PrP mutants incapable of undergoing N-glycosylation (WT^{nG}-, $E196K^{nG}$-, $E200K^{nG}$-, and $E219K^{nG}$-PrPs), in which Asn at the two *N*-glycosylation sites were changed to Thr. When expressed in K-041 cells, these non-glycosylated PrPs exhibited similar mobility shifts to those of PNGase F-treated PrPs (compare Fig. 3B and 3C). These variant-dependent mobility shifts were unlikely to have been due to artifacts that may have occurred during or after cell lysis because the fixation of cells by TCA prior to cell lysis did not affect the mobility of mutant PrPs (Fig. 4B). The mobility shifts of the E196K and E200K mutant PrPs in SDS-PAGE were not affected by their exposure to chaotropic reagents such as urea and GdnHCl (Fig. 4A and 4B), suggesting that the shifts were not due to the difference in conformations of PrPs in SDS-PAGE. The mechanisms responsible for mobility shifts have not yet been elucidated. Previous biophysical and biochemical analyses demonstrated that WT-, E196K-, and E200K-PrPs had similar overall thermodynamic stabilities, while slight differences may exist in the intramolecular interactions of several amino acid residues or solvent accessibility of the surface of PrP.[25–28] Thus, subtle local electrostatic differences among E196K-, E200K-, and E219K-PrPs may affect electrophoretic mobility; however, these three PrPs had equal net charges after the E-to-K substitution.

In the present study, we established the human neuroblastoma cell line K-041, which lacked endogenous *PRNP*. K-041 cells enabled us to analyze PrP variants associated with human hereditary prion diseases in the absence of possible interfering effects by endogenous PrP.

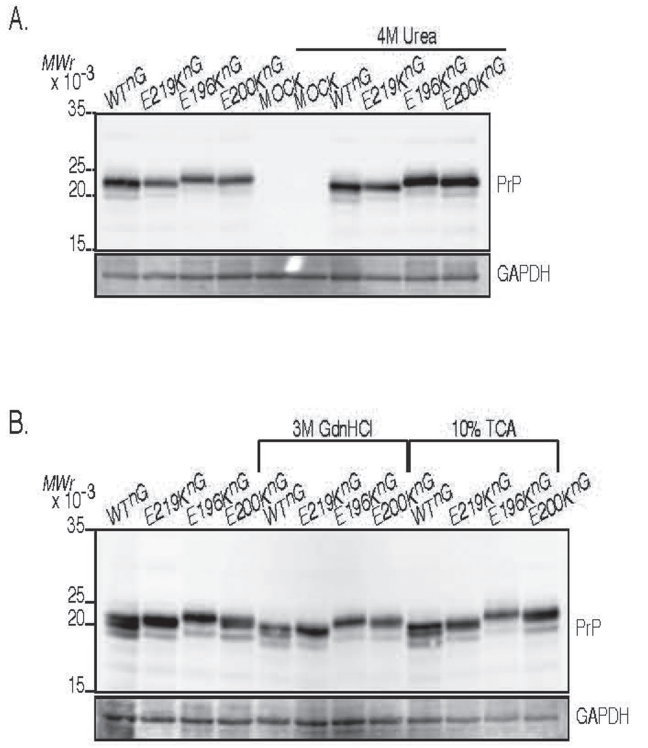

Fig. 4. Electrophoretic Mobility of the Non-Glycosylated form of PrPs after a Treatment by Urea and GdnHCl.

Non-glycosylated PrPs were transiently expressed in K-041 cells. Cell lysates were treated with 4 M urea (A) or 3 M GdnHCl (B) before SDS-PAGE. Alternatively, cells were fixed with 10% TCA to inactivate cellular enzymes before lysis in NP40-DOC buffer, and lysates were applied to SDS-PAGE (B).

Acknowledgments This work was supported by AMED under Grant Number JP16ek0109044j and MEXT KAKENHI Grant Number 17H04003.

Conflict of interest The authors declare no conflict of interest.

REFERENCES

1) Oesch B, Westaway D, Walchli M, McKinley MP, Kent SB, Aebersold R, Barry RA, Tempst P, Teplow DB, Hood LE, *et al*. A cellular gene encodes scrapie PrP 27-30 protein. *Cell*, **40**, 735–746 (1985).
2) Vilette D. Cell models of prion infection. *Vet. Res.*, **39**, 10 (2008).
3) Mehrabian M, Brethour D, MacIsaac S, Kim JK, Gunawardana CG, Wang H, Schmitt-Ulms G. CRISPR-Cas9-based knockout of the prion protein and its effect on the proteome. *PLoS One*, **9**, e114594 (2014).
4) Sakudo A, Onodera T. Prion protein (PrP) gene-knockout cell lines: insight into functions of the PrP. *Front. Cell Dev. Biol.*, **2**, 75 (2014).
5) Collinge J. Prion diseases of humans and animals: their causes and molecular basis. *Annu. Rev. Neurosci.*, **24**, 519–550 (2001).
6) Beck JA, Poulter M, Campbell TA, Adamson G, Uphill JB, Guerreiro R, Jackson GS, Stevens JC, Manji H, Collinge J, Mead S. *PRNP* allelic series from 19 years of prion protein gene sequencing at the MRC Prion Unit. *Hum. Mutat.*, **31**, E1551–E1563 (2010).
7) Bagyinszky E, Giau VV, Youn YC, An SSA, Kim S. Characterization of mutations in *PRNP* (prion) gene and their possible roles in neurodegenerative diseases. *Neuropsychiatr. Dis. Treat.*, **14**, 2067–2085 (2018).
8) Goldgaber D, Goldfarb LG, Brown P, Asher DM, Brown WT, Lin S, Teener JW, Feinstone SM, Rubenstein R, Kascsak RJ, *et al*. Mutations in familial Creutzfeldt-Jakob disease and Gerstmann-Sträussler-Scheinker's syndrome. *Exp. Neurol.*, **106**, 204–206 (1989).
9) Spudich S, Mastrianni JA, Wrensch M, Gabizon R, Meiner Z, Kahana I, Rosenmann H, Kahana E, Prusiner SB. Complete penetrance of Creutzfeldt-Jakob disease in Libyan Jews carrying the E200K mutation in the prion protein gene. *Mol. Med.*, **1**, 607–613 (1995).
10) Cong L, Ran FA, Cox D, Lin S, Barretto R, Habib N, Hsu PD, Wu X, Jiang W, Marraffini LA, Zhang F. Multiplex genome engineering using CRISPR/Cas systems. *Science*, **339**, 819–823 (2013).
11) Cadinanos J, Bradley A. Generation of an inducible and optimized piggyBac transposon system. *Nucleic Acids Res.*, **35**, e87 (2007).
12) Zhao S, Jiang E, Chen S, Gu Y, Shangguan AJ, Lv T, Luo L, Yu Z. PiggyBac transposon vectors: the tools of the human gene encoding. *Transl. Lung Cancer Res.*, **5**, 120–125 (2016).
13) Pocchiari M, Puopolo M, Croes EA, Budka H, Gelpi E, Collins S, Lewis V, Sutcliffe T, Guilivi A, Delasnerie-Laupretre N, Brandel JP, Alperovitch A, Zerr I, Poser S, Kretzschmar HA, Ladogana A, Rietvald I, Mitrova E, Martinez-Martin P, de Pedro-Cuesta J, Glatzel M, Aguzzi A, Cooper S, Mackenzie J, van Duijn CM, Will RG. Predictors of survival in sporadic Creutzfeldt-Jakob disease and other human transmissible spongiform encephalopathies. *Brain*, **127**, 2348–2359 (2004).
14) Büeler H, Fischer M, Lang Y, Bluethmann H, Lipp HP, DeArmond SJ, Prusiner SB, Aguet M, Weissmann C. Normal development and behaviour of mice lacking the neuronal cell-surface PrP protein. *Nature*, **356**, 577–582 (1992).
15) Manson JC, Clarke AR, Hooper ML, Aitchison L, McConnell I, Hope J. 129/Ola mice carrying a null mutation in PrP that abolishes mRNA production are developmentally normal. *Mol. Neurobiol.*, **8**, 121–127 (1994).
16) Kuwahara C, Takeuchi AM, Nishimura T, Haraguchi K, Kubosaki A, Matsumoto Y, Saeki K, Yokoyama T, Itohara S, Onodera T. Prions prevent neuronal cell-line death. *Nature*, **400**, 225–226 (1999).
17) Peoc'h K, Manivet P, Beaudry P, Attane F, Besson G, Hannequin D, Delasnerie-Lauprêtre N, Laplanche JL. Identification of three novel mutations (E196K, V203I, E211Q) in the prion protein gene (*PRNP*) in inherited prion diseases with Creutzfeldt-Jakob disease phenotype. *Hum. Mutat.*, **15**, 482 (2000).
18) Shi Q, Chen C, Song XN, Gao C, Tian C, Zhou W, Song XH, Yao LS, Han J, Dong XP. A Chinese Creutzfeldt-Jakob disease patient with E196K mutation in *PRNP*. *Prion*, **5**, 117–120 (2011).
19) Rudd PM, Wormald MR, Wing DR, Prusiner SB, Dwek RA. Prion glycoprotein: structure, dynamics, and roles for the sugars. *Biochemistry*, **40**, 3759–3766 (2001).
20) Baskakov IV, Katorcha E, Makarava N. Prion strain-specific structure and pathology: a view from the perspective of glycobiology. *Viruses*, **10**, 723 (2018).
21) Harris DA, Gorodinsky A, Lehmann S, Moulder K, Shyng SL. Cell biology of the prion protein. *Curr. Top. Microbiol. Immunol.*, **207**, 77–93 (1996).
22) Prusiner SB, Scott MR, DeArmond SJ, Cohen FE. Prion protein biology. *Cell*, **93**, 337–348 (1998).
23) Zaidi SI, Richardson SL, Capellari S, Song L, Smith MA, Ghetti B, Sy MS, Gambetti P, Petersen RB. Characterization of the F198S prion protein mutation: enhanced glycosylation and defective refolding. *J. Alzheimers Dis.*, **7**, 159–171, discussion, 173–180 (2005).
24) Capellari S, Parchi P, Russo CM, Sanford J, Sy MS, Gambetti P, Petersen RB. Effect of the E200K mutation on prion protein metabolism. Comparative study of a cell model and human brain. *Am. J. Pathol.*, **157**, 613–622 (2000).
25) Liemann S, Glockshuber R. Influence of amino acid substitutions related to inherited human prion diseases on the thermodynamic stability of the cellular prion protein. *Biochemistry*, **38**, 3258–3267 (1999).
26) Hasegawa K, Mohri S, Yokoyama T. Fragment molecular orbital calculations reveal that the E200K mutation markedly alters local structural stability in the human prion protein. *Prion*, **4**, 38–44 (2010).
27) Rossetti G, Giachin G, Legname G, Carloni P. Structural facets of disease-linked human prion protein mutants: a molecular dynamic study. *Proteins*, **78**, 3270–3280 (2010).
28) Meli M, Gasset M, Colombo G. Dynamic diagnosis of familial prion diseases supports the β2-α2 loop as a universal interference target. *PLoS One*, **6**, e19093 (2011).